Pure & Appl. Chem., Vol. 57, No. 11, pp. 1659–1665, 1985.
Printed in Great Britain.

Evaluation of fiber surface treatments in composite materials

A.T. DiBenedetto

Institute of Materials Science, University of Connecticut
Storrs, Connecticut 06268

Abstract - The physical properties of fiber reinforced composite materials depend on the ability of the polymer matrix both to transmit stresses to the fiber reinforcement and to protect the fibers from damage. To promote these characteristics, fibers are treated during manufacture with mixtures of sizing and coupling agents. The optimization of a given coating is complicated by the fact that individual components often perform more than one function. An experimental technique and a theoretical analysis have been developed which allow evaluation of both the stress transfer capability and the fiber protection performance of a given surface treatment. The analysis should be of particular value in the optimization of commercial fiber treatments.

INTRODUCTION

There is considerable interest in composite materials of plastics reinforced with high strength fibers such as glass and graphite. Among the many reasons is the possibility of fabricating materials for use in structures that, on the basis of weight, are stronger and more rigid than those using conventional materials of construction. For example, a plastic reinforced with fifty percent by volume of a continuous, high modulus graphite fiber, oriented in one direction, can attain a modulus of elasticity and a tensile strength of the same order as those of high strength steel, at least in the direction of the oriented fibers. Since such a composite weighs approximately one-fifth that of steel, the specific properties, such as the modulus of elasticity and strength per unit of specific gravity, are five times greater for the composite material.

The properties of a composite material depend on the behavior of its constituent parts as well as that of the interfaces between reinforcement and matrix. Strength, toughness, fatigue resistance, and the life expectancy of the composite are particularly sensitive to the stability and strength of the interfaces. For example, the absence of adhesion between fiber and matrix will invariably lead to low strength. Also, if the chemical bonding between phases is not strong, environmental agents such as water can migrate to the interfaces, destroy the initial adhesion, and cause degradation of strength properties.

The anisotropic nature of fiber reinforced composite materials leads to characteristics which are not ordinarily found in the traditional isotropic materials of construction. Even if the fibers are randomly oriented so that the material is isotropic on a macroscopic scale, locally there is anisotropy in the regions around individual fibers. Strength and rigidity are high in a direction parallel to a fiber axis, but fall to the level of those of the plastic perpendicular to the axis. The angular dependence of properties is strongly dependent upon the adhesion between the two phases. Generally, in order to promote high performance and long term stability, it is necessary to form high strength, chemically stable interfaces between the fiber and plastic components (1).

Because of the need to transfer stress from the matrix to the reinforcement, the reinforcing phase must have a relatively high ratio of fiber length to diameter. High strength, high modulus reinforcing fibers such as glass or graphite, however, are brittle materials which are susceptible to severeproperty deterioration and breakage due to surface damage during handling and composite manufacture. In order both to protect the fibers and to promote high fiber-matrix adhesion, mixtures of sizing and coupling agents are applied to the fiber surfaces during the fiber manufacturing process. The function of a sizing agent is to protect the fiber from surface abrasion caused by handling and fiber-fiber contacts. For example, a glass fiber might be coated with a thin polymeric film of polyvinyl acetate (PVA) in order to minimize surface abrasion and protect against the damaging effects of humidity. The function of a coupling agent is to promote fiber-matrix adhesion, but when used in sufficient quantity also to serve as a protective coating. A coupling agent is any substance which can interact chemically or physically with both the fiber surface and the

polymer matrix. The most effective and widely used coupling agents for glass fibers are the organosilanes having the general structure, X_3SiR. The R group is chosen to be resinophilic. It may be vinyl, γ-methacryloxy-propyl, γ-amino propyl, etc., depending upon the reactivity of the polymer phase. The X-groups are usually methoxy, ethoxy or chloro. The X-groups hydrolyze in the presence of water to form silanols which in turn can either condense with the silanols present on the glass surface to form siloxane linkages with the glass or can condense with each other to form a siloxane polymer coating on the surface. Interactions other than chemical reaction can also occur between the coupling agent and the surfaces. For example, silane molecules can hydrogen bond to the surface, rather than covalently bond. One theory suggests a mechanism that involves a reversible silanol bond formation and a dynamic equilibrium of the coupling agent competing with small penetrant molecules such as water (2).

Interesting studies of molecular interactions at interfaces have utilized spectroscopic techniques such as Auger electron spectroscopy, nuclear magnetic resonance spectroscopy and infra-red and laser Raman spectroscopy. Although the sensitivity and selectivity of these techniques have been problematic, they provide direct evidence of the interactions on a molecular level. For example, both laser Raman spectroscopy and Fourier Transform infra-red spectroscopy have been used to demonstrate chemical reaction between silanes and styrene monomers (3). When styrene monomers were polymerized on methacry-silane-treated glass fibers the styrene spectrum was identical to that of the homopolymer, but the carbonyl stretching frequency at 1718 cm^{-1} of the unreacted silane shifted to 1702 cm^{-1} after the polymerization. This indicates that styrene was homopolymerized and grafted to the silane at the chain end. In another study, infra-red spectroscopy was employed to give evidence of a chemical reaction between polyethylene and vinyltriethoxysilane (4).

In addition to chemical reaction at coupling agent/matrix interfaces, the presence of fiber surfaces can modify the morphology of the matrix phase, thus causing significant changes in the physical properties of the matrix. For example, infra-red spectroscopy has been used to show that glass fibers will preferentially adsorb an amine catalyst from an epoxy resin, thus changing the cure rate and the morphology of the resin surrounding the fiber (5). In another study, nuclear magnetic resonance was used to characterize the change of relaxation properties of a phenoxy resin at silicate surfaces (6). These are only a few examples of the many spectroscopic studies reported in the literature.

In a composite material the fiber is imbedded in the polymer matrix. The mechanical function of the interfaces is to transmit stresses from the weak, deformable polymer matrix to the strong, rigid fiber. The ability to transmit stress will be limited by either the shear strength of the matrix, the adhesive strength of the matrix/fiber interface, or the load bearing capacity of the fibers. In evaluating composite performance it is necessary to locate the weakest link in the system and to determine the failure mechanism. It is not yet possible to predict the failure mechanism from spectroscopic data on the interface, so one must resort to mechanical tests for evaluation.

The traditional method of evaluating a composite material by mechanical testing under various conditions of temperature and environment measures only the overall fiber reinforcement efficiency and is not capable of distinguishing the effects of fiber/matrix interaction vis-a-vis improved fiber protection. Recognizing the need for improved fiber treatment evaluation procedures, several investigators have used an experimental technique and theoretical analysis to evaluate both the stress transfer capability and the fiber protection performance of a given fiber treatment formulation (7, 8, 9).

In this presentation, the technique is described and the results of such a test are used to calculate the value of a parameter, τ, which measures the stress-transfer capability of a given fiber treatment when the fiber is completely encapsulated in a polymer matrix. The ability of the surface treatment to protect the fiber from surface damage is evaluated by measuring the tensile strength of the fiber as a function of its length. This procedure may be used for the routine screening and evaluation of new fiber surface treatments and, furthermore, by correlating the measured parameters with other composite properties, such as strength, toughness, impact strength and fatigue resistance, one may more reliably optimize these properties in a given composite material. Experimental evidence will be presented which illustrates the efficacy of the proposed technique.

THE FIBER FRAGMENTATION TEST: A MEASURE OF STRESS TRANSFER IN COMPOSITES

A single fiber encapsulated in a compression molded test specimen in the form of a dumbell is used in the test. A single fiber is mounted on a fork and placed in the cavity of a mold which is filled with the encapsulating matrix. The samples are either formed under heat and pressure or cast, as appropriate. The samples are subjected to traction in a tensile-testing machine to an elongation greater than that required to fracture the fibers. (The matrix material must have an elongation-to-break greater than that of the fiber.)

Since the volume fraction of fiber material in the sample is less than the critical value, the fiber will break into many small fragments (10). The lengths of these fragments are a measure of the ability of the interface to transmit the imposed stresses from the matrix to the fiber. If the sample is not transparent, the matrix must be dissolved or pyrolized in order to measure the distribution of fiber fragment lengths. The lengths of the fiber fragments are measured using a projection microscope of low amplification. The fragments are classified according to their lengths and a cumulative distribution of lengths is calculated. The relation between the distribution of fragment lengths and the ability of the interface to transmit stresses depends on the mechanism of stress transfer between phases.

Figure 1 shows schematically a fiber implanted in a resin. The traction stress, applied externally, is transferred to the fiber by means of a shear stress across the interface. The tensile stress in the fiber increases from nearly zero at the fiber ends to a maximum value, limited by the breaking stress of the fiber. When this limit is reached, the fiber breaks at its weakest point. If it is not long enough, the fiber cannot break since the generated tensile stress cannot reach its maximum value. The fiber length for which the generated tensile stress reaches a value of the breaking strength of the fiber exactly at the midpoint of the length is called the "critical length," ℓ_c. Kelly and Tyson (10) have related the critical length ℓ_c to the yield stress of the matrix at the interface τ through a force balance around the imbedded fiber. They assumed that the shear stress at the interface is constant and equal to the yield strength of the matrix or the "resistance" of the interface and obtained the following equation for the critical length:

$$\ell_c = \frac{\sigma_f \, d_f}{2 \tau_y} \tag{1}$$

where σ_f is the average breaking strength of the fiber, d_f is fiber diameter and τ_y is the shear strength of the interface. Thus if one measures the breaking strength of the fiber, one can estimate an effective interfacial strength τ_y from the critical length ℓ_c.

When a specimen containing a single fiber is subjected to tensile deformation and the plastic matrix deforms beyond the elongation-to-break of the fiber, the fiber will break at its weakest point as illustrated schematically in Fig. 2. At this point one has two pieces of fiber of different lengths. Under continued deformation, the fiber stress continues to increase until it reaches the breaking stress of one of the two fragments, at which point a second fracture occurs. This process will continue until all of the fragments are smaller than their critical lengths, after which fiber fracture is no longer possible. When a fiber of length ℓ_c is fractured, two pieces of length $\ell_c/2$ should be obtained. The Kelly-Tyson model predicts that the fiber fracture process should result in a distribution of fragment lengths from $\ell_c/2$ to ℓ_c. If the tensile strength of the fiber is independent of fiber length, one may calculate an effective interfacial shear strength τ_y from the measured critical length, using equation 1. Often, the distribution of fragment lengths obtained is broader than the 2:1 ratio predicted by the Kelly-Tyson model. This has been attributed to the variation of breaking strength with fiber length (8).

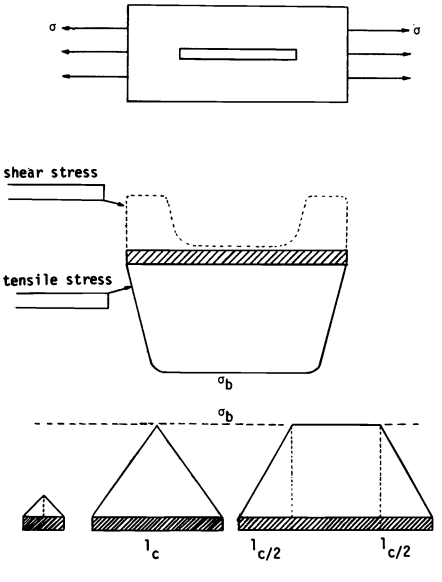

Fig. 1. Stress-Transfer Mechanism in Short Fiber Reinforced Composites

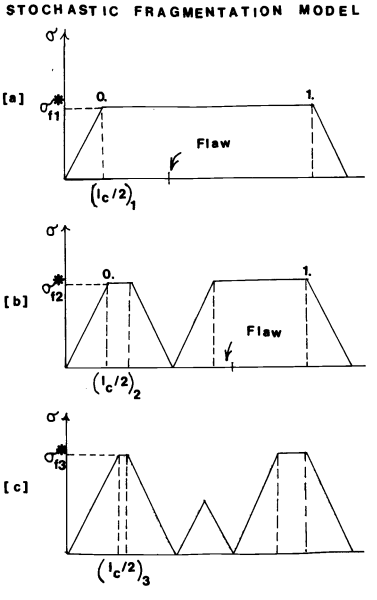

Fig. 2. The stochastic fiber fragmentation model.

An estimate of an "effective" interfacial strength, τ_e, may be obtained from the midpoint of the cumulative distribution curve (i.e., at P = 0.5) where the experimental fragment length is approximately 3/4 (ℓ_c). Using equation (1), one may estimate a value of τ_e from the median critical length $(\ell_c)_m$ and the mean tensile strength at that length, (σ_m) :

$$\tau_e \doteq \frac{3\sigma_m d_f}{8(\ell_c)_m} \tag{2}$$

A more accurate measure of the stress transferability, τ, can be obtained by taking into account the variation of fiber tensile strength with length. A bilinear logarithmic strength-length behavior has been observed for glass fibers and has been simulated in terms of a "weakest-link" model of a chain of n elements of length ℓ_o (11). Our analysis uses a double box distribution function, from which one can express the average strength as a function of fiber length L and five model parameters:

$$\langle\sigma\rangle = f(L, \sigma_1, \sigma_2, \sigma_4, p, \lambda = \ell_o/p) \tag{3}$$

where p is the fraction of elements containing a severe flaw, σ_1 is a lower limiting strength of a continuous fiber, σ_2 is the lower limiting strength of a continuous fiber not containing a severe flaw, σ_4 is the theoretical strength of a flaw-free fiber, and λ is the average distance between severe flaws on the fiber.

COMPUTER SIMULATION OF THE FIBER FRAGMENTATION TEST

An embedded single filament contains flaws randomly along its length. Thus, when the sample undergoes tensile deformation, a sequence of fiber fractures occurs randomly along the effective length of the fiber. This process is simulated by using a random generator to choose sites for the sequential fractures (8). One starts with a single filament of given length and diameter embedded in a resin matrix. The average breaking strength of the fiber $\langle\sigma\rangle_1$, is computed using Eq. 3 for a set of model parameters. Upon tensile deformation, the tensile stress in the fiber builds up from zero at the ends to a value $\langle\sigma\rangle_1$ in the interior. The "ineffective" lengths $(\ell_c/2)_1$ at the fiber ends can be calculated from Eq. 1, assuming a first value for τ. Excluding the ineffective fiber ends as potential fracture sites, the computer selects a random number, between 0 and 1, which fixes the location for the first fracture site, as illustrated in Fig. 2a.

Since the process is stochastic, the second fracture might occur in either of the two fragments.

A second random number is generated, which fixes the position of the second fracture. When a fragment is formed that is smaller than the current critical fiber length, it cannot undergo further fragmentation and is decoupled from the system. This is schematically shown in Fig. 2c. Stochastic fragmentation of the remaining fragments, controlled by the random number generation, continues until all fiber fragments are shorter than the current critical length. At this point, the total number of fragments are counted to assess whether this constitutes enough for a distribution curve (200-300 fragments). If not, the process is initiated on a new length of fiber with the model parameters unchanged. Fragments are accumulated until a theoretical fragment-length distribution is adequately defined.

Both the mean position of the distribution and the extent of dispersion depend on both the magnitude of the interfacial shear strength and the strength properties of the fibers. Written in its most general form, the model generates a cumulative distribution of critical aspect ratios (i.e. ℓ_c/d_f) as a function of five strength parameters and the interfacial shear strength:

$$P(\ell_c/d_f) = f(\sigma_1, \sigma_2, \sigma_4, p, \lambda, \tau) \tag{4}$$

The next step in the analysis is to obtain values for the parameters using available experimental data.

ANALYSIS OF EXPERIMENTAL DATA

In theory one should be able to use the technique of constrained non-linear optimization to obtain optimized values for the six model parameters from an experimental fragment length distribution curve. At best, optimization in six dimensions is extremely difficult, so we choose to estimate three of the strength parameters from measurements of the mean fiber strength at three different gage lengths. Furthermore, σ_4, the theoretical strength of flaw-free glass, was set at 1.5×10^6 psi. (In any case the magnitude of this parameter has little effect on the final results). The optimization problem is thereby reduced to a two-dimensional search for λ and τ:

$$P(\ell_c/d_f) = f(\lambda, \tau) \tag{5}$$

RESULTS

Experiments were conducted using specially extruded and coated E-glass fibers from both Owens-Corning and P.P.G. Industries (8). The average strengths of single filaments at different gage lengths were determined using ASTM D3379-75 as standard, and are shown in Tables 1 and 2. The matrices used were nylon 6, high-density polyethylene, polypropylene and an acid-grafted polypropylene.

TABLE 1. Properties of the Owens-Corning E-glass Fiber Strands

Treatment[1]	<σ> 0.25 in. (psi)	<σ> 1.0 in. (psi)	<σ> 3.0 in. (psi)
None	332,460	237,600	182,150
0.5 wt% PVA (0.47% actual)	355,030	277,660	228,520
0.2% A-1100 (0.17 actual)	373,300	302,190	255,600
0.2% A-1100+ 0.5% PVA (0.75 total actual)	359,780	270,010	215,080

1. PVA = polyvinyl acetate sizing agent
A-1100 = Union Carbide's λ-amino propyltriethoxy silane

TABLE 2. Properties of PPG E-glass Fiber Strands

Treatment[1]	<σ> 0.25 in. (psi)	<σ>[2] 1.0 in. (psi)	<σ>[2] 3.0 in. (psi)
None	232,510	143,440	97,820
0.10 wt% A-174	317,470	237,980	165,470
0.33% A-174	368,570	319,670	285,570
0.57% PVA/LUB	340,900	259,440	209,250
0.8% A-174/PVA/LUB	281,480	206,570	194,700
1.02% A-174/PVA/LUB	383,040	303,550	252,450

1. A-174 = Union Carbide's λ-methacryloxy propyl triethyoxysilane
LUB = Cirrasol 185 A CH_3 $(CH_2)_8$ $CONH_2$
2. Calculated from Weibull parameters at 0.25 in. fiber length

The cumulative fiber fragment data were obtained on tensile specimens containing a single 3-inch continuous filament.

The tensile specimens were stretched to approximately their yield elongation. They were then placed in a pyrex glass petri dish and pyrolyzed on a hot plate until the resin was transformed into a carbonized char. The dishes were then placed in a muffle furnace to complete the ashing. The recovered fiber fragments were measured using a low-power Nikon projection microscope. Fragments, normalized by their diameter, were ranked according to size, and the cumulative frequency distribution was evaluated. The ashing of unstretched bars resulted in the recovery of filaments greater than 1 inch in length.

Optimized values for the model parameters were obtained using the procedure outlined above. A typical result for the Owens-Corning E-glass fiber coated with 0.2 percent A-1100 and embedded in Nylon 6 is illustrated in Fig. 3. One can see that the "theoretical" distribution describes well the experimental distribution. Table 3 presents the values obtained for model parameters. The optimized shear strength λ decreases with temperature, but at all

TABLE 3. Results for E-glass Fibers in Nylon 6

	τ (psi)				λ	σ_1	σ_2
Treatment	25°C	75°C	125°C	175°C	(in)	(psi)	(psi)
None	4260	3800	3200	2200	0.38	151,100	396,600
0.5% PVA	4800	3800	2800	2100	0.42	200,130	404,700
0.5% PVA/ 0.2% A-1100	4600	3800	2900	2600	0.41	183,800	417,200
0.2% A-1100	5000	3900	3700	2700	0.43	228,200	416,000
Yield Strength of Nylon 6 (Dry) in Shear (psi)	7000	5100	4000	3100			

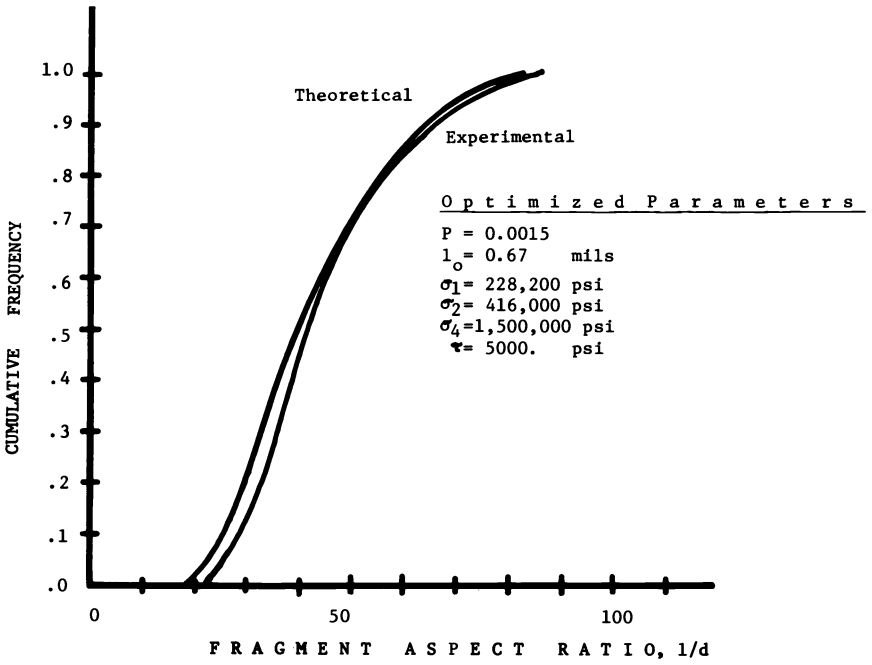

Fig. 3. Experimental and optimized theoretical ℓ/d distribution curves for the Owens-Corning E-glass fiber coated with 0.2 weight percent A-1100 in nylon 6 (dry) at 25°C.

temperatures it is of the order 60 to 90 percent of the shear yield strength of the nylon matrix, indicating that the yield strength of the nylon matrix probably is the limiting factor rather than the strength of the interface. The severe flaw separation λ is of the order of 0.38 to 0.43 inches and is independent of temperature.

The A-1100 treated fibers had the highest values for the shear-transmission parameter τ, at all temperatures. The two coatings containing PVA show a distinct softening between 75 and 125°C, probably associated with the low-glass-transmition temperature of polyvinyl acetate. The A-1100 coated fibers maintain a level of stress transfer of 70 percent of the yield strength at low temperature to 90 percent of the yield strength at higher temperature, where the nylon is less notch-sensitive. With the untreated fibers, the level varies from about 60 to 70 percent of the yield strength over the same temperature range, perhaps indicating a tendency for frictional slippage at the fiber-matrix interface. Somewhat unexpectedly, the A-1100 coated fibers also had the highest strength. The PVA sizing agent did not appear to protect the fibers against damage to the same extent as a good coating of silane. The untreated fibers, as expected, produce the poorest composite properties.

The result for PPG E-glass fibers in high density polyethylene, and also in polypropylene are shown in Tables 4 and 5. The coating of 0.33 percent A-174 (γ-methacryloxy propylsilane) appears to give the best fiber protection; fibers coated with a mixture of PVA, polyvinyl acetate , and lubricant (Cirrasol 185 A $CH_3(CH_2)_8CONH_2$) appear to be somewhat weaker. The methacryloxy silane, when used alone, appears to provide good shear transmission between the high-density polyethylene and the glass fibers. The optimized value of 2000 psi is of the order of the yield strength of the polyethylene. It is probable

TABLE 4. PPG E-glass in HDPE at 25°C

Treatment	τ(psi)	λ(in.)	σ_1(psi)
0.33% A-174	2000	0.47	264,900
0.57% PVA/LUB	500	0.40	181,100
0.80% A-174/PVA/ LUB	440	0.39	136,300
1.02% A-174/PVA/ LUB	700	0.43	222,600

TABLE 5. PPG E-glass in Polypropylene at 25°C

Treatment	τ(psi)	λ(in.)	σ_1(psi)
None	930	0.32	73,340
0.1% A-174	710	0.40	161,760
0.33% A-174	675	0.47	264,900
0.57% PVA/LUB	1085	0.40	181,100
0.80% A-174/PVA/ LUB	860	0.39	136,300
1.02% A-174/PVA/ LUB	1120	0.43	222,600

Table 6. Commercial E-glass Strands in Various Thermoplastics at 25°C

Treatment	Resin	τ(psi)	λ(in.)	σ_1(psi)
A-1100/PVA/LUB	Nylon 6 (dry)	4,500	0.39	145,300
1.6wt%	Polypropylene	890		
A-1100	Acid Grafted	3,000	0.44	221,850
3.0wt%	Polypropylene			
	Polypropylene	950		

that the silane reacts chemically with the polyethylene and that the PVA/Lub combination interferes with that reaction. None of the treatments appear to provide significant shear transmission in polypropylene.

When the shear transmission is good, the theoretical and experimental cumulative distribution curves are well matched, but when the shear transmission is at the level of the frictional forces, the experimental distribution is broader than the theoretical. Optical evidence indicates a stick-slip shearing at the interface under these conditions.

The results for commercially available E-glass fibers in Nylon 6 and polypropylene in one case and acid-grafted polypropylene and unmodified polypropylene in the other are illustrated in Table 6. The fiber parameters were similar to those for the specially prepared fibers and the heavier surface coating of the amino silane by itself seemed to provide better protection against damage. In both cases, the shear transmission parameter in polypropylene was of the order of 900 psi or 1/3 of the matrix shear strength, indicating transmission primarily through friction. In contrast the Nylon 6 at 4500 psi (or 65 percent of yield shear strength) and the acid-grafted polypropylene at 3000 psi (100 percent of yield shear strength) exhibited better stress transmission. Once again when the shear transmissibility is good, the cumulative distributions are narrow, the mean values of aspect ratio are low, and the optimized fits represent the data very well. When the shear transmissibility is poor, the cumulative distributions are broader, the mean values of aspect ratio are higher, and the theoretical curves are narrower than the experimental data.

CONCLUSIONS

A simple embedded single filament test has been developed which allows evaluation of both the stress transfer capability of a fiber-matrix interface and the fiber protection performance of a given fiber treatment. Since the experimental technique and associated analysis can separate coupling and sizing effects of fiber surface treatments, they should be of particular value in the optimization of commercial fiber treatments.

REFERENCES

1. L.J. Broutman, R.H. Krock, Eds., Composite Materials, 6, Chapter #1 by P.W. Erickson & E.P. Plueddemann, Academic Press, New York, (1974).
2. E.P. Plueddemann, Modern Plastics, 47, 92, (1970).
3. H. Ishida, G. Kumar (Eds.), Molecular Characterization of Composite Interfaces, Plenum Press, New York, (1985).
4. M.S. Akutin, et al., Mekhanika Polimerov, 8, 1048 (1972).
5. P.W. Erickson, Proc. 25th Annual Tech. Conf., Reinforced Plastics Div., SPI, Section 13-A (1970).
6. D.H. Droste, A.T. DiBenedetto, E.O. Stejskal, J. Polymer Science, Part 2A, 9, 187, (1971).
7. L. Ongchin, W.K. Olender and F.H. Ancker, Proc. 27th Conf. SPI Reinforced Plastics Div., Sec. 11-A (1972).
8. W.A. Fraser, F.H. Ancker, A.T. DiBenedetto, B. Elbirli, Polymer Composites, 4, no. 4, 238, Oct. (1983).
9. L.T. Drzal, M.J. Rich, J.D. Camping, W.J. Park, Proceedings 35th Annual Tech. Conf. Reinforced Plastics Div. SPI, Section 20-C, 1, (1980).
10. A. Kelly, W.R. Tyson, J. Mech. Phys. Solids, 13, 329 (1965).
11. B.W. Rosen "Mechanics of Composite Strengthening", Chapter 3 in Fiber Composite Materials, ASM, Metals Park, Ohio (1965).